

# MicroRNA-378 attenuates myocardial fibrosis by inhibiting MAPK/ERK pathway

W.-Y. LIU<sup>1</sup>, H.-H. SUN<sup>2</sup>, P.-F. SUN<sup>1</sup>

<sup>1</sup>Department of Cardiovascular Surgery, The Affiliated Yantai Yuhuangding Hospital of Qingdao University, Yantai, China

<sup>2</sup>Department of Intensive Care Unit, The Affiliated Yantai Yuhuangding Hospital of Qingdao University, Yantai, China

*Wenyi Liu and Haihong Sun contributed equally to this article*

**Abstract.** – **OBJECTIVE:** To elucidate the role of microRNA-378-containing microvesicles (MVs) in the process of myocardial fibrosis and its underlying mechanism.

**MATERIALS AND METHODS:** *In vivo* chronic myocardial fibrosis (MF) model in rats was established by aortic coarctation method. MicroRNA-378 mimic or inhibitor was injected into the rat tail vein at day 3 after the aortic coarctation. Two weeks later, rats were sacrificed for collecting myocardium. MVs were isolated from rat cardiomyocytes and further verified by detecting the expression level of its marker CD63. Expression levels of fibrosis-related indicators and microRNA-378 in MVs were determined by quantitative Real Time-Polymerase Chain Reaction (qRT-PCR) and Western blot. After induction with transforming growth factor- $\beta$ 1 (TGF- $\beta$ 1) in primary rat cardiomyocytes for different time points, expression levels of fibrosis-related indicators and microRNA-378 were also accessed. Changes in mitogen-activated protein kinase (MAPK) pathway were observed during the process of MF by qRT-PCR and Western blot.

**RESULTS:** Expression levels of microRNA-378-containing MVs decreased, and the MAPK pathway was activated during the process of MF, which further aggravated MF.

**CONCLUSIONS:** MicroRNA-378-containing MVs alleviate myocardial fibrosis through inhibiting the phosphorylation of MAPK.

*Key Words:*

Microvesicles, MicroRNA-378, MAPK, Myocardial fibrosis.

## Introduction

With the society development, living standard improvement and lifestyle changes, the prevalence and mortality of cardiovascular diseases are on

the rise. In China, the incidence of cardiovascular disease is about 20%, and its mortality accounts for as high as 40%. It is estimated that the prevalence of cardiovascular diseases will continue to increase in the next decade rapidly. Cardiovascular diseases not only pose serious burdens on affected patients and their families, but also influence social and economic development. Therefore, it is particularly urgent to search for efficient prevention and treatment methods of cardiovascular diseases.

Regardless of the pathogenic causes of cardiovascular diseases, the common pathological outcome is myocardial fibrosis in the late stage. Myocardial fibrosis (MF) manifests as cardiomyocyte proliferation and excessive deposition of extracellular matrix in the myocardium<sup>1,2</sup>. MF is an essential cause of ventricular remodeling<sup>3</sup>. Its pathological performances include increased myocardial stiffness, decreased myocardial contractility, and reduced coronary flow reserve, eventually causing myocardial ischemia, and even malignant arrhythmia and sudden death<sup>4</sup>.

However, the specific pathogenesis of MF has not been well elucidated so far. A large number of studies<sup>5-8</sup> have shown that transgenic growth factors, inflammatory factors, renin-angiotensin-aldosterone system, regulatory cytokines, oxidative stress, endothelial dysfunction, intracellular calcium, and other factors are responsible for the pathogenesis of MF. These factors influence the occurrence and development of MF through various pathways. There are many cell-cell communication methods, among which, microvesicles (MVs) have been concerned in recent years<sup>9</sup>. MVs are widely present in living organisms, and secreted by almost all cells in mammals. MVs contain a

variety of biological information substances, such as proteins, lipids, nucleic acids, ions, etc., and they transmit information to target cells through the ligand-receptor. MVs are proved to regulate cardiovascular disease<sup>10,11</sup>, immune escape of tumor cells<sup>12</sup>, renal interstitial fibrosis<sup>13-15</sup>, and foeto-maternal communication<sup>16</sup>.

MicroRNAs are a class of endogenous, non-coding single-stranded RNAs of approximately 22 nucleotides in length<sup>17</sup>. They are widely found in eukaryotes. It is reported that microRNAs are able to regulate one-third of human genes. Previous researches on microRNA-regulated apoptosis were mainly focused on tumor cells<sup>18</sup>. Recently, the crucial function of microRNAs in tissue fibrosis has been increasingly recognized. MicroRNA-378 exerts its biological role in the process of liver, lung, kidney, and myocardial fibrosis<sup>19-22</sup>. It affects intercellular communication mainly through mitogen-activated protein kinase/extracellular regulated protein kinases (MAPK/ERK) pathway. Therefore, we hypothesized that microRNA-378 participates in the development of MF through the MAPK/ERK pathway. We specifically explored the possible mechanism of MF in this study, which will bring new therapeutic targets for the treatment of chronic ischemic heart diseases.

## Materials and Methods

### Animals

Male Wistar rats in clean level weighing 245-320 g were obtained from the Experimental Animal Center of Nanjing University and were given to normal diet and water. Rats were randomly assigned into sham group, AC 1 w group, AC 2 w group, and AC 3 w group, with 4 rats in each group. Rat myocardium was harvested at postoperative 1, 2 and 4 weeks, respectively. This study was approved by the Animal Ethics Committee of Qingdao University Animal Center.

### Aortic Coarctation Procedures

Rats were fasted 12 hours before surgery. They were intraperitoneally anesthetized with 10% chloral hydrate (0.4 mL/100 g) and placed on the surgical table. The abdominal aorta was fully exposed by opening the left upper abdomen and ligated 0.5 cm above both sides of renal arteries with the needle. Subsequently, the needle was removed, and the abdominal aorta was expected to

narrow by about 50%-60%. Rats in sham group were only cut open without performing ligation. The postoperative intramuscular injection of 50000 U penicillin was performed to prevent infection.

### MicroRNA-378 Overexpression or Knockdown in Rats

A full-length expression plasmid (1 mg/kg) dissolved in 2 mL of saline was quickly injected into the rat tail vein in 10 s at day 3 after the aortic coarctation. Rats in N.C. group were administered with the pcDNA3.1 diluted in the same volume of saline. Two weeks later, rats were sacrificed for harvesting myocardial tissues.

### Culture of Primary Rat Cardiomyocytes

Culture medium: PriCells Medium + 10% fetal bovine serum (FBS; Gibco, Rockville, MD, USA) + 1% P/S + PriCells Supplement. Washing buffer: 1 × phosphate-buffered saline (PBS) (pH 7.4) + 1% P/S. Digestion solution: PriCells Isolation of Primary Cell Kit. Briefly, hearts of neonatal rats with 1-3 days old were harvested and washed in the washing buffer. The atria was collected and washed until the washing buffer was clear. Subsequently, the atria was cut into 1 mm<sup>3</sup> tissue and digested in 10 mL of digestion solution at 37°C water bath for 8 min. The remaining tissues were continually digested for another 10 min after discarding the supernatant for 3-5 times. The terminated digestion solution was centrifuged at 1000 rpm/min for 10 min, and cells were cultured in a bottle at a density of  $5 \times 10^5$ /mL.

### MVs Isolation and Observation

MVs were isolated from cell supernatant by ultracentrifugation. Briefly, cell culture was collected and centrifuged at 4°C, 300 g/min for 5 min, 1,200 g/min for 20 min, and 10,000 g/min for 30 min sequentially. The suspension was harvested for centrifugation again at 110,000 g/min for 60 min and the precipitate was MVs. MVs were resuspended in PBS and observed using the transmission electron microscope.

### Western Blot

Total protein was extracted for determining protein concentration. After being separated by sodium dodecyl sulphate-polyacrylamide gel electrophoresis (SDS-PAGE), proteins were transferred to the membrane and blocked with 5% skim milk for 1 hour. The specific primary

antibody was used to incubate with the membrane overnight at 4°C. After being washed with 1 × tris buffered saline-tween (TBST) for 5 times, the secondary antibody was used to incubate the membrane for 2 h at room temperature. After washing with 1×TBST for 1 min, the chemiluminescent substrate kit was used for exposure of the protein band. Primary antibodies used here were: FN (cat: 3648, Sigma-Aldrich, St. Louis, MO, USA),  $\alpha$ -SMA (cat: 5691, Sigma-Aldrich, St. Louis, MO, USA), COL-1 (cat: 34710, Abcam, Cambridge, MA, USA), p-MAPK (cat: 126425, Abcam, Cambridge, MA, USA), CD63 (cat: ab59479, Abcam, Cambridge, MA, USA) and actin (cat: sc1616, Santa Cruz Biotechnology, Santa Cruz, CA, USA).

#### **Quantitative Real Time-Polymerase Chain Reaction (qRT-PCR)**

We used TRIzol (Invitrogen, Carlsbad, CA, USA) to extract total RNA from cells or tissues for reverse transcription according to the instructions of PrimeScript RT reagent Kit (TaKaRa, Otsu, Shiga, Japan). 1  $\mu$ L of complementary deoxyribose nucleic acid (cDNA) was collected for PCR using SYBR Green method. CT value was recorded through ABI7300 system (Applied Biosystems, Foster City, CA, USA) and the relative gene expression was calculated with  $2^{\Delta CT}$  method. Primer sequences used in this study were as follows: FN, F: 5'-CCAG-GAACCCTCCTTACTC-3', R: 5'-ACTAGG-GTGTGTCCGAAGGA-3'; microRNA-378, F: 5'-GGCCTGTAAACATCCTCGACTG-3', R: 5'-ATGTCGTGGTGCGTAGTCG-3'; COL-1, F: 5'-ATTACAGCGGCATTTGGACAA-3', R: 5'-CGTATAGCGACAGTTCGCGAT-3';  $\alpha$ -SMA, F: 5'-ATTACCCGGCATTGGACAA-3', R: 5'-TTAACCGAATAGCGACAGTTCT-3'; CD63: F: CACGCTCTCACCTCTGTCTACTG, R: GCTACGGGGGCTTGCTACT; p-MAPK: F: CAGCTGGAGAGTGTGCCTGCG, R: GGTGT-GTGCTCTGCTTGAGACT; U6: F: 5'-GCTTCG-GCAGCACATATACTAAAAT-3', R: 5'-CGCT-TCAGAATTTGCGTGTCAT-3'; GAPDH: F: 5'-CGCTCTCTGCTCCTCCTGTTC-3', R: 5'-ATCCGTTGACTCCGACCTTCAC-3'.

#### **Echocardiography**

Rats were anesthetized with intraperitoneal injection of sodium pentobarbital (0.04 g/kg) and placed in a supine position on a wooden board with 30° to the left. The chest area was depilated, and connected with ECG II. A ULTRAMARK 9 ultrasound instrument connected with a wi-

de-band linear array probe (10 MHz to 5 MHz) was used here. The detection frequency was 6.0 MHz, the probe length was 38 mm and the image depth was 2.5 cm. The probe was placed on the left side of the sternum, with 10° to 30° from the midline of the sternum, showing the long axis of the left ventricle of the sternum. The short axis of the left ventricle of the sternum would be shown when the probe was rotated 90° clockwise. Doppler flow detection was performed at mitral, aortic and pulmonary valves at the angle of 18°, 50°, and 2°, respectively. The sampling volume was 1 mm. Clear images were captured for subsequent analyses.

#### **Ultrasonic Measurement Index**

Left ventricular end-diastolic anterior wall thickness (AWT), posterior wall thickness (PWT), left ventricular end-diastolic diameter (LVDd), and left ventricular end-systolic diameter (LVDs) were recorded. Left ventricular end-diastolic volume (LVEDV) and left ventricular end-systolic volume (LVESV) were calculated from the left internal diameter (D) according to the formula  $V=1.04 \times D^3$ . Stroke volume (SV) = LVEDV-LVESV. Left ventricular ejection fraction (EF) = SV / LVEDV × 100%.

#### **Transfection**

Cells were seeded in a 6-well plate with the serum-containing medium. Until 90-95% of cell fusion, 1.5 mL of serum-free medium was replaced per well. 2.5  $\mu$ g of plasmid DNA and 5  $\mu$ L of Lipofectamine 2000 (Invitrogen, Carlsbad, CA, USA) were diluted with 250  $\mu$ L Opti-MEM, respectively, and incubated for 5 min at room temperature. After mixture and maintenance at room temperature for 20 min, 500  $\mu$ L of the transfection mixture was added to each well. The medium was replaced 6 h later. Cells induced with or without transforming growth factor- $\beta$ 1 (TGF- $\beta$ 1) were collected 48 hours later.

#### **Statistical Analysis**

Statistical Product and Service Solutions (SPSS) 16.0 statistical software (SPSS Inc., Chicago, IL, USA) was used for data analysis. Measurement data were expressed as mean  $\pm$  standard deviation ( $\bar{x} \pm s$ ). Comparison of measurement data was conducted using the *t*-test. Comparison of differences among each group was conducted using one-way ANOVA, followed by Post-Hoc Test (Least Significant Difference).  $p < 0.05$  was considered statistically significant.

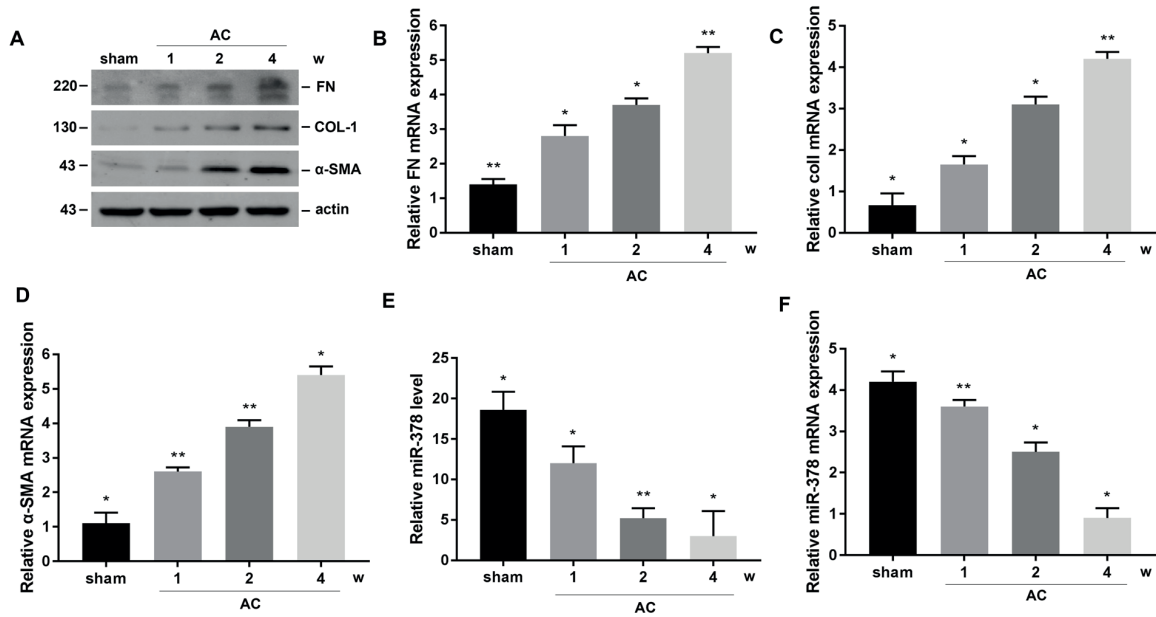


**Figure 1.** MicroRNA-378 expression decreased in MF rats. **A**, Western blot analyses of FN, COL-1, and  $\alpha$ -SMA in rat myocardium. **B-D**, The mRNA levels of FN (**B**), COL-1 (**C**), and  $\alpha$ -SMA (**D**) in rat myocardium. **E**, Relative expression of microRNA-378 in rat myocardium. **F**, The mRNA level of microRNA-378 in rat myocardium. \* $p$ <0.05, \*\* $p$ <0.01.

## Results

### MicroRNA-378 Expression Decreased in MF Rats

First of all, a chronic MF model in rats was established by aortic coarctation method. Rats were sacrificed for harvesting myocardial tissues at postoperative 1, 2, and 4 weeks, respectively. Expression levels of fibrosis-related indicators in rat myocardium were determined. Compared with sham group, protein expressions of FN, collagen I (COL-1), and  $\alpha$ -SMA in MF rats gradually increased with the prolongation of MF (Figure 1B). Identically, mRNA levels of FN, COL-1, and  $\alpha$ -SMA in rat myocardium also increased in a time-dependent manner (Figure 1B-D). Subsequently, microRNA-378 expression was determined in rat myocardium at postoperative 1, 2, and 4 weeks, respectively. Its expression gradually decreased in a time-dependent manner after aortic coarctation (Figure 1E and 1F). The above results indicated downregulation of microRNA-378 expression in MF rats.

### TGF- $\beta$ 1 Induced Phenotypic Changes in Primary Rat Cardiomyocytes

Primary rat cardiomyocytes were induced with 5 ng/mL TGF- $\beta$ 1 for 12 h, 24 h, and 48 h, respectively. Western blot results indicated that protein levels of FN, COL-1, and  $\alpha$ -SMA were

time-dependently elevated (Figure 2A). In the process of MF, we suspected that the amount of signaling-containing MVs increased. Therefore, we extracted MVs in culture medium and verified by detecting the protein expression of CD63 (a marker of MVs) using Western blot. With the prolongation of TGF- $\beta$ 1 induction, the protein level of CD63 was gradually elevated in primary rat cardiomyocytes (Figure 2B). The mRNA level of CD63 showed the similar trend, revealing the increased amount of MVs (Figure 2C). MicroRNA-378 transmits cell-cell information through MVs. Subsequently, we detected the mRNA expression of microRNA-378 in MVs extracted from the same volume of culture medium, and found that microRNA-378 expression gradually decreased with the prolongation TGF- $\beta$ 1 induction (Figure 2D). The above results elucidated that microRNA-378 expression in MVs decreased during the process of TGF- $\beta$ 1-induced MF.

### MicroRNA-378 Overexpression Elevated EF and Inhibited MF

To elucidate the regulatory effect of microRNA-378 on the development of MF, we administered microRNA-378 mimic or inhibitor in rat tail vein after aortic coarctation for consecutive three days. Transfection efficacy of microRNA-378 mimic and inhibitor was first verified by qRT-PCR (Figure 3A).

Two weeks after aortic coarctation, the left ventricular ejection fraction (EF%) of rats was measured by echocardiography. Rats injected with microRNA-378 mimic showed higher EF% than controls, whereas those injected with microRNA-378 inhibitor had much lower EF%. Rat myocardium was harvested after plasmids administration for two weeks. Western blot results revealed higher protein expressions of FN and  $\alpha$ -SMA in the myocardium of rats injected with microRNA-378 inhibitor, whereas those overexpressing microRNA-378 showed downregulated FN and  $\alpha$ -SMA (Figure 3C). The mRNA levels of FN and  $\alpha$ -SMA in rats administrated with microRNA-378 mimic or inhibitor presented the same trends as their protein levels (Figure 3D and 3E). Therefore, we hypothesized that overexpression of microRNA-378 alleviated MF.

### Inhibition of MAPK Pathway Alleviated MF

Previous studies have shown that inhibition of the MAPK pathway can alleviate renal interstitial fibrosis<sup>21</sup>. We thereafter speculated whether the

regulatory effect of microRNA-378 on the development of MF relied on the MAPK pathway inhibition in cardiomyocytes. First, we found that the protein level of p-MAPK remarkably increased at 2 weeks after aortic coarctation (Figure 4A). The mRNA level of p-MAPK was identically elevated (Figure 4B). *In vitro* experiments showed upregulation of p-MAPK in primary rat cardiomyocytes with TGF- $\beta$ 1 induction for 48 h (Figure 4C). The mRNA level of p-MAPK in TGF- $\beta$ 1-induced cardiomyocytes increased as well (Figure 4D). Similarly, both protein and mRNA levels of p-MAPK pronouncedly increased in rats administrated with microRNA-378 inhibitor (Figure 4E and 4F). The above results indicated that microRNA-378 attenuated MF by inhibiting MAPK pathway.

### Discussion

Heart failure is the end-stage performance of various cardiovascular diseases. Its high morbidi-

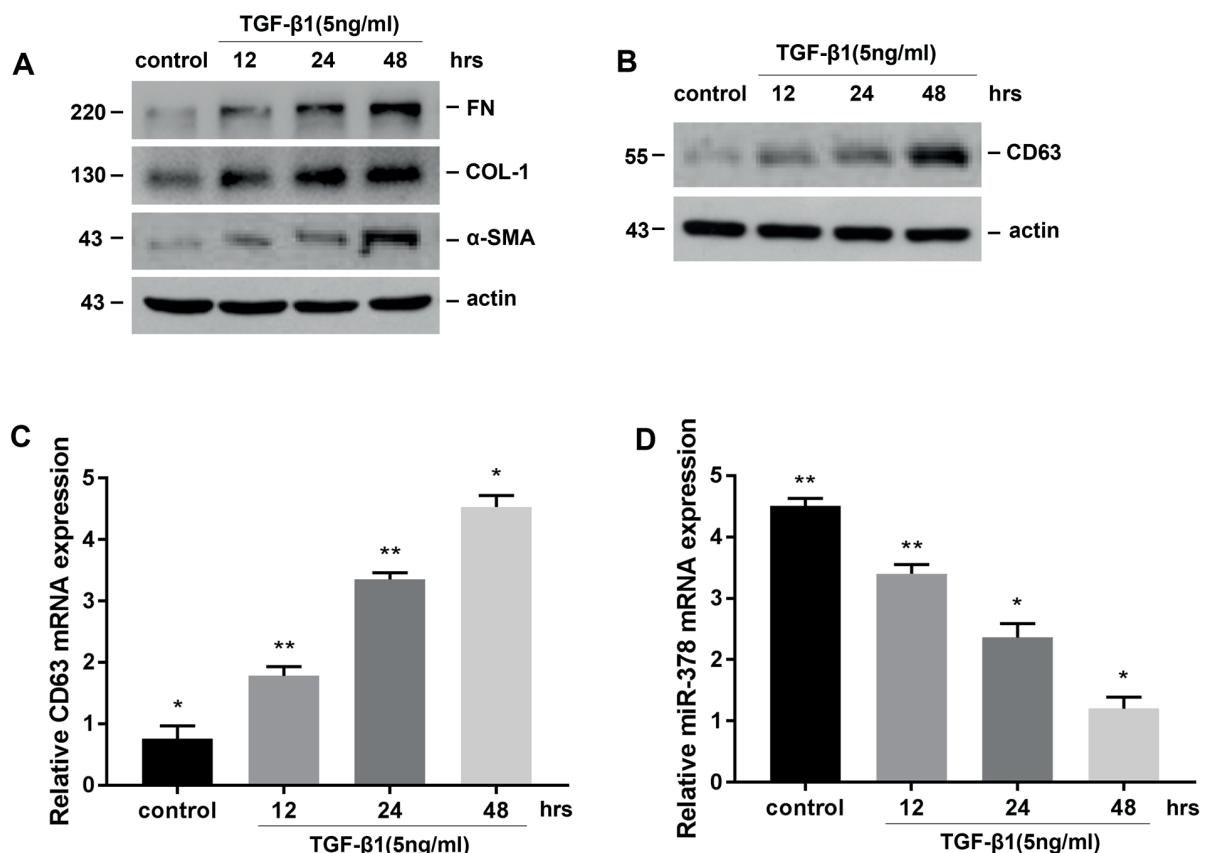


**Figure 2.** TGF- $\beta$ 1 induced phenotypic changes in primary rat cardiomyocytes. Primary rat cardiomyocytes were induced with 5 ng/mL TGF- $\beta$ 1 for 12 h, 24 h, and 48 h, respectively. **A**, Western blot analyses of FN, COL-1, and  $\alpha$ -SMA. **B**, Western blot analysis of CD63. **C**, The mRNA level of CD63. **D**, The mRNA level of microRNA-378. \* $P$ <0.05, \*\* $P$ <0.01.

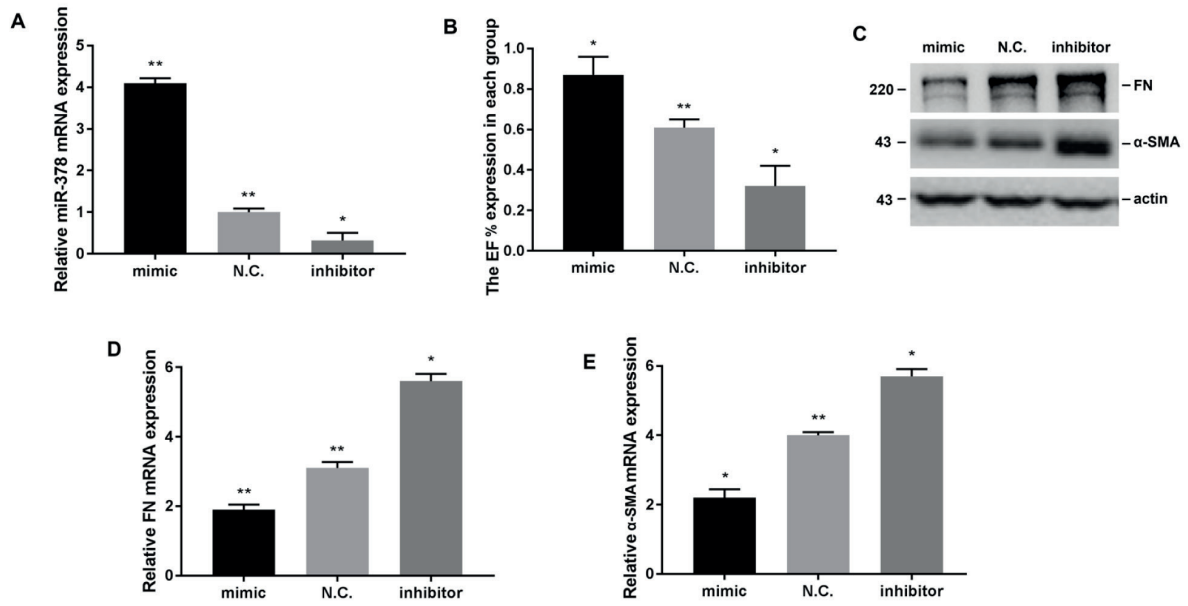


**Figure 3.** MicroRNA-378 overexpression elevated EF and inhibited MF. **A**, Transfection efficacy of microRNA-378 mimic and inhibitor was first verified by qRT-PCR. **B**, EF (%) in rats administrated with microRNA-378 mimic or inhibitor. **C**, Western blot analyses of FN and  $\alpha$ -SMA in rats administrated with microRNA-378 mimic or inhibitor. **D**, The mRNA level of FN in rats administrated with microRNA-378 mimic or inhibitor. **E**, The mRNA level of  $\alpha$ -SMA in rats administrated with microRNA-378 mimic or inhibitor. \* $p$ <0.05, \*\* $p$ <0.01.

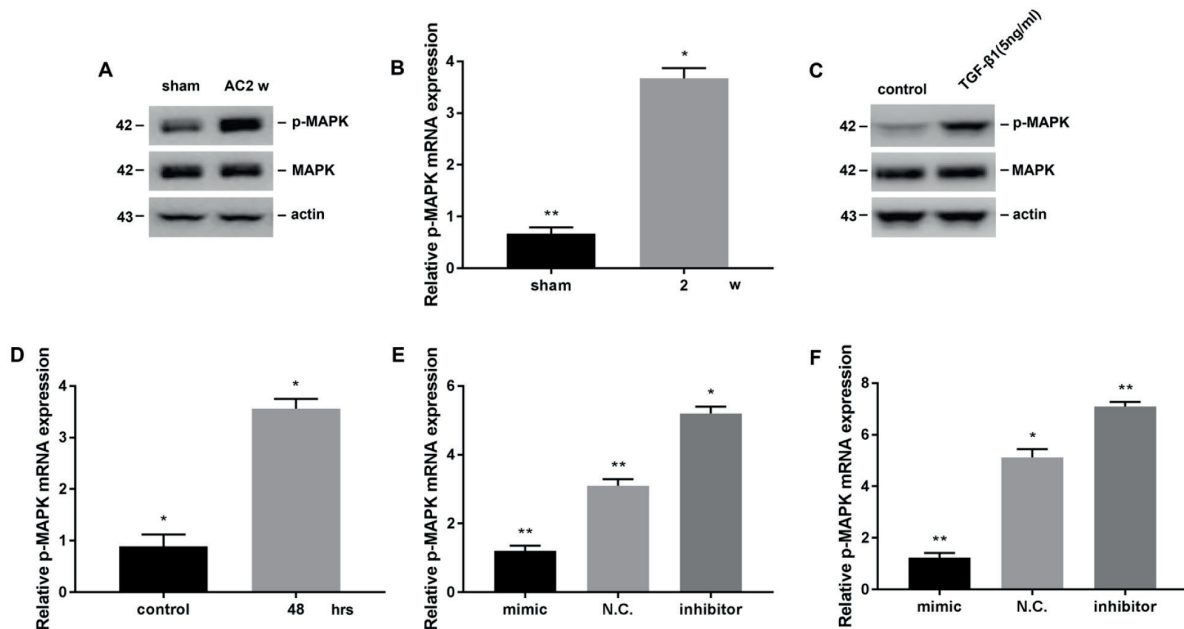


**Figure 4.** Inhibition of the MAPK pathway alleviated MF. **A**, Western blot analyses of p-MAPK and MAPK in rats at two weeks after aortic coarctation. **B**, The mRNA level of p-MAPK in rats at two weeks after aortic coarctation. **C**, Western blot analyses of p-MAPK and MAPK in rats at two weeks after TGF- $\beta$ 1. **D**, The mRNA level of p-MAPK in primary rat cardiomyocytes with TGF- $\beta$ 1 induction for 48 h. **E-F**, Relative expression of p-MAPK in rats administrated with microRNA-378 mimic or inhibitor. \* $p$ <0.05, \*\* $p$ <0.01.

ty and mortality seriously affect the life quality of affected patients. Therefore, prevention and treatment of cardiovascular diseases are hotspots in cardiovascular researches.

MF is the common pathological outcome in a certain stage of cardiovascular diseases<sup>23</sup>. Current researches<sup>24,25</sup> demonstrated that multiple factors may be explained for the pathogenesis of MF. Pathophysiological processes, molecular biology, and drug intervention of MF are the research focuses. Myocardial ischemia model, aortic coarctation model, and chronic emergency model are usually utilized as the *in vivo* MF model in experimental researches. This study established the *in vivo* chronic MF model in rats by aortic coarctation method and *in vitro* MF model by TGF- $\beta$ 1 induction in primary rat cardiomyocytes, to observe expression changes in fibrosis markers and microRNA-378.

MAPK is a highly conserved pathway involved in various cellular functions, including cell proliferation, differentiation, and migration, especially in tumor formation and migration. Previous studies<sup>19-22</sup> have shown that potential function of microRNA-378 in tissue fibrosis is achieved by activating the MAPK pathway. We, therefore, hypothesized that microRNA-378 is involved in MF by activating this pathway. MicroRNA-378 mimic and inhibitor were constructed. Changes in expressions of relative genes in the MAPK pathway further verified our idea.

The shortcoming of this investigation was that we only established the aortic coarctation model for elucidating the potential mechanism of MF. Whether similar biological effects have existed in other MF models are needed to be further explored.

## Conclusions

We showed that microRNA-378-containing MVs alleviate myocardial fibrosis through inhibiting the phosphorylation of MAPK.

## Conflict of interest

The authors declare no conflicts of interest.

## References

- 1) DANIELS A, VAN BILSEN M, GOLDSCHMEDING R, VAN DER VUSSE GJ, VAN NIEUWENHOVEN FA. Connective tissue growth factor and cardiac fibrosis. *Acta Physiol (Oxf)* 2009; 195: 321-338.
- 2) MARTOS R, BAUGH J, LEDWIDGE M, O'LOUGHLIN C, CONLON C, PATLE A, DONNELLY SC, McDONALD K. Diastolic heart failure: evidence of increased myocardial collagen turnover linked to diastolic dysfunction. *Circulation* 2007; 115: 888-895.
- 3) WEBER KT, SUN Y, BHATTACHARYA SK, AHOKAS RA, GERLING IC. Myofibroblast-mediated mechanisms of pathological remodelling of the heart. *Nat Rev Cardiol* 2013; 10: 15-26.
- 4) CHEN L, XIA W, HOU M. Mesenchymal stem cells attenuate doxorubicin-induced cellular senescence through the VEGF/Notch/TGF $\beta$  signaling pathway in H9c2 cardiomyocytes. *Int J Mol Med* 2018; 42: 674-684.
- 5) CHUNG CC, HSU RC, KAO YH, LIOU JP, LU YY, CHEN YJ. Androgen attenuates cardiac fibroblasts activations through modulations of transforming growth factor-beta and angiotensin II signaling. *Int J Cardiol* 2014; 176: 386-393.
- 6) CHEN L, XIA W, HOU M. Mesenchymal stem cells attenuate doxorubicin-induced cellular senescence through the VEGF/Notch/TGF $\beta$  signaling pathway in H9c2 cardiomyocytes. *Int J Mol Med* 2018; 42: 674-684.
- 7) AONUMA T, TAKEHARA N, MARUYAMA K, KABARA M, MATSUKI M, YAMAUCHI A, KAWABE J, HASEBE N. Apoptosis-resistant cardiac progenitor cells modified with apurinic/aprimidinic endonuclease/redox factor 1 gene overexpression regulate cardiac repair after myocardial infarction. *Stem Cells Transl Med* 2016; 5: 1067-1078.
- 8) SALVARANI N, MAGUY A, DE SIMONE SA, MIRAGOLI M, JOUSSET F, ROHR S. TGF- $\beta$ 1 (Transforming Growth Factor-beta1) plays a pivotal role in cardiac myofibroblast arrhythmogenicity. *Circ Arrhythm Electrophysiol* 2017; 10: e4567.
- 9) RATAJCZAK J, WYSOCZYNSKI M, HAYEK F, JANOWSKA-WIECZOREK A, RATAJCZAK MZ. Membrane-derived microvesicles: important and underappreciated mediators of cell-to-cell communication. *Leukemia* 2006; 20: 1487-1495.
- 10) AYERS L, NIEUWLAND R, KOHLER M, KRAENKEL N, FERRY B, LEESON P. Dynamic microvesicle release and clearance within the cardiovascular system: triggers and mechanisms. *Clin Sci (Lond)* 2015; 129: 915-931.
- 11) POE AJ, KNOWLTON AA. Exosomes as agents of change in the cardiovascular system. *J Mol Cell Cardiol* 2017; 111: 40-50.
- 12) TAYLOR DD, GERCEL-TAYLOR C. Exosomes/microvesicles: mediators of cancer-associated immunosuppressive microenvironments. *Semin Immunopathol* 2011; 33: 441-454.
- 13) HE J, WANG Y, LU X, ZHU B, PEI X, WU J, ZHAO W. Micro-vesicles derived from bone marrow stem cells protect the kidney both in vivo and in vitro by microRNA-dependent repairing. *Nephrology (Carlton)* 2015; 20: 591-600.
- 14) BORGES FT, MELO SA, OZDEMIR BC, KATO N, REVUELTA I, MILLER CA, GATTONE VN, LEBLEU VS, KALLURI R. TGF- $\beta$ 1-containing exosomes from injured epithelial cells activate fibroblasts to initiate tissue

- regenerative responses and fibrosis. *J Am Soc Nephrol* 2013; 24: 385-392.
- 15) ZHENG SB, ZHENG Y, JIN LW, ZHOU ZH, LI ZY. Microvesicles containing microRNA-21 secreted by proximal tubular epithelial cells are involved in renal interstitial fibrosis by activating AKT pathway. *Eur Rev Med Pharmacol Sci* 2018; 22: 707-714.
  - 16) TONG M, KLEFFMANN T, PRADHAN S, JOHANSSON CL, DE-SOUSA J, STONE PR, JAMES JL, CHEN Q, CHAMLEY LW. Proteomic characterization of macro-, micro- and nano-extracellular vesicles derived from the same first trimester placenta: relevance for fetomaternal communication. *Hum Reprod* 2016; 31: 687-699.
  - 17) LEE RC, FEINBAUM RL, AMBROS V. The *C. elegans* heterochronic gene *lin-4* encodes small RNAs with antisense complementarity to *lin-14*. *Cell* 1993; 75: 843-854.
  - 18) WANG Y, LEE CG. MicroRNA and cancer-focus on apoptosis. *J Cell Mol Med* 2009; 13: 12-23.
  - 19) ZHANG T, HU J, WANG X, ZHAO X, LI Z, NIU J, STEER CJ, ZHENG G, SONG G. MicroRNA-378 promotes hepatic inflammation and fibrosis via modulation of the NF- $\kappa$ B-TNF $\alpha$  pathway. *J Hepatol* 2018:
  - 20) HYUN J, WANG S, KIM J, RAO KM, PARK SY, CHUNG I, HACS, KIM SW, YUN YH, JUNG Y. MicroRNA-378 limits activation of hepatic stellate cells and liver fibrosis by suppressing Gli3 expression. *Nat Commun* 2016; 7: 10993.
  - 21) WANG B, YAO K, WISE AF, LAU R, SHEN HH, TESCH GH, RICARDO SD. miR-378 reduces mesangial hypertrophy and kidney tubular fibrosis via MAPK signalling. *Clin Sci (Lond)* 2017; 131: 411-423.
  - 22) NAGALINGAM RS, SUNDARESAN NR, NOOR M, GUPTA MP, SOLARO RJ, GUPTA M. Deficiency of cardiomyocyte-specific microRNA-378 contributes to the development of cardiac fibrosis involving a transforming growth factor beta (TGF $\beta$ 1)-dependent paracrine mechanism. *J Biol Chem* 2014; 289: 27199-27214.
  - 23) ISTRATOAIIE O, OFITERU AM, NICOLA GC, RADU RI, FLORESCU C, MOGOANTA L, STREBA CT. Myocardial interstitial fibrosis - histological and immunohistochemical aspects. *Rom J Morphol Embryol* 2015; 56: 1473-1480.
  - 24) GUO Y, GUPTA M, UMBARKAR P, SINGH AP, SUI JY, FORCE T, LAL H. Entanglement of GSK-3 $\beta$ ,  $\beta$ -catenin and TGF- $\beta$ 1 signaling network to regulate myocardial fibrosis. *J Mol Cell Cardiol* 2017; 110: 109-120.
  - 25) LIANG B, XIAO T, LONG J, LIU M, LI Z, LIU S, YANG J. Hydrogen sulfide alleviates myocardial fibrosis in mice with alcoholic cardiomyopathy by downregulating autophagy. *Int J Mol Med* 2017; 40: 1781-1791.